

## **QUICK CORE ASSESSMENT FROM CT IMAGING: FROM PETROPHYSICAL PROPERTIES TO LOG EVALUATION**

Olivier Lopez, Carl F. Berg, Lars Rennan, Gunnar Digranes, Thibaut Forest, Anders Kristoffersen & Bjarne R. Bøklepp.  
Statoil ASA, Research center (Rotvoll, Norway)

*This paper was prepared for presentation at the International Symposium of the Society of Core Analysts held in Snowmass, Colorado, USA, 21-26 August 2016*

### **ABSTRACT**

Computerized tomography (CT) is now widely used in the oil and gas industry, both for imaging of multiphase core flooding experiments and for rock characterization. Recent advances in CT scanners have greatly decreased the acquisition time and increased the image quality, rendering it possible to scan full cored intervals within a short timeframe (hours). Core properties such as bulk density (RHOB), mean atomic number (Zeff) and photo electric factor (PEF) can be derived directly from CT scans performed at two different energy levels (DECT).

In this study, we will present a new way to integrate CT images and data in log evaluation software. Several hundreds of meters of core originating from multiple fields have been scanned in different commercial laboratories using dual energy technique. Scanning parameters have been standardized for better reproducibility and comparison between fields. All the cores are scanned on arrival in the laboratory within their barrel before any operation is performed on them. Primary evaluations are used to ensure coring quality and for seal peel selection. Acquired 3D CT volumes are then further processed to extract 2D images: unwrapped surface and longitudinal slices.

All the 2D CT images are aligned and oriented using newly developed libraries in VirtualCore software and then exported as compatible file format for log evaluation software (DLIS). The resulting images have been incorporated as image logs for calibration, QA/QC and interpretation of existing borehole image logs (QuantaGeo, OBMI, UBI). Dip picking and fracture orientation have been performed on the oriented high resolution images,

In addition to images, derived properties (RHOB) have been used for calibrating and interpreting logging while drilling (LWD) logs for thin bedded and laminated intervals where the resolution of the logging tool was not sufficient to capture existing heterogeneities.

## INTRODUCTION

Computerized tomography (CT) imaging has been used in the oil industry for decades [1, 2]. Typical uses include inspection of cores to evaluate plug drilling location, inspection of plug samples before further analysis, imaging of core flooding experiments [3,4], and rock characterization [5, 6, 7, 8] This paper will concentrate on developments in rock characterization, and then especially as an extension to more traditional log evaluation.

3D volumes obtained from the CT scans cannot be easily integrated with log evaluation software and are often used outside regular workflows. Extracting selected 2D images from 3D volumes makes it possible to integrate the density based information from CT into log evaluation software alongside other dataset.

Such extensions of CT imaging use have been spurred by advances in CT scanners and reconstruction algorithms. In the last decade the image quality has been improved alongside a significant reduction in acquisition time. It is now possible to scan full cored intervals within timeframes that does not obstruct the traditional core handling workflows significantly.

Dual energy CT-scanning (DECT) is scanning the same location twice with different X-ray energies. The attenuation of X-rays is a function of both electron density and effective atomic number. For high energies the X-ray attenuation is dominated by Compton scattering which responds to density changes, while at low energies photo-electric effects which responds to the effective atomic number becomes more predominant [2]. Due to the speed of the CT scanners, the extra time involved in scanning the core samples twice at two different energy levels is small compared to the time needed to load and unload the samples.

In this paper we present a workflow integrating images and derived properties from DECT into common commercially available log evaluation software. We have developed scripts to automatically integrate CT images into available log evaluation software. This includes orientation of the CT images according to borehole image logs. Calculations of derived properties are sensitive to the scanning equipment, and we have investigated calibration routines for different types of reservoir rocks. We then compared the generated results with data acquired from conventional logging suites.

## BACKGROUND

A CT scanner consists of an X-ray source and detectors. The X-rays penetrate the sample from different angles; either by rotating the source or the sample, and the detectors records the transmitted X-ray intensity. The X-ray attenuation is described by Beer's law:

$$\frac{I}{I_0} = e^{-\mu h}, \quad (1)$$

where  $I_0$  is the X-ray intensity before and  $I$  is the intensity after passing through a volume element of length  $h$  in the direction of the X-ray, and  $\mu$  is the attenuation coefficient of the material. Assuming Beer's law in each basic volume quantity (voxel), it is possible to back-calculate the attenuation  $\mu_r(x)$  for each position (voxel)  $x$  in the sample based on the aggregate attenuations for the different paths between the source and the detectors.

For medical scanners it is typical to normalize the attenuation values  $\mu_r(x)$  by the attenuation of water,  $\mu_w$ , e.g. yielding the attenuation as dimensionless:

$$\mu(x) = 1000 \frac{\mu_r(x)}{\mu_w}, \quad (2)$$

This then gives an attenuation value close to 1000 for water, while air is little X-ray attenuating and therefore obtains values close to 0.

For high X-ray energies the attenuation is dominated by Compton scattering, while at lower energy levels the photoelectric effect becomes more dominant. This change in how the X-rays interact with the matter for different energy levels leads to a dependency on density,  $\rho$ , and atomic number,  $Z$ , described by the function

$$\mu = \rho \left( a + b \frac{Z^{3.8}}{E^{3.2}} \right), \quad (3)$$

where  $a$  is assumed to be little influenced by the energy level,  $b$  is a constant, and  $E$  is the energy level. From this equation we see that for high energy levels the attenuation coefficient will be dominated by the density, while at lower energy levels the influence of the atomic number will increase.

This energy dependence enables estimation of the density by the following linear equations [9]:

$$\rho = \alpha \mu_l + \beta \mu_h + \gamma. \quad (4)$$

Here  $\alpha, \beta$  and  $\gamma$  are constants that needs to be calibrated, while  $\mu_l$  and  $\mu_h$  are the attenuation coefficients for low and high energy scans, respectively. Similarly, one obtains this linear equation for the photo electric factor:

$$P_e = \frac{1}{10} \left( \frac{\delta \mu_l + \epsilon \mu_h + \zeta}{0.9342\rho + 0.1759} \right), \quad (5)$$

Here  $\delta$ ,  $\epsilon$  and  $\zeta$  are constants that needs to be calibrated. The last two equations will be used in this paper to calculate the density and photoelectric factor on core samples.

From the density calculated in Equation 4, we can estimate the total porosity based on fluid assumptions using the following equation:

$$\phi_t = \frac{\rho_m - \rho}{\rho_m - \rho_f} \quad (6)$$

Where  $\phi_t$  is the total porosity,  $\rho$  is the density from DECT,  $\rho_m$  is an estimate for the matrix density and  $\rho_f$  is an estimate for the fluid density. We note that this estimate is dependent on your choice for matrix and fluid density, in addition to the uncertainty in the calculated density value from DECT.

## METHODS

### Calibration:

The Compton scattering is predominant for X-ray energies above 100kV, while photoelectric absorption is dominant well below 100 kV [2]. To enhance the effect of the different interaction between X-ray and matter, one would like to have energy levels well above and below 100kV. Our medical scanner has a maximal energy level of 140kV, so we used this energy level for the high energy scans. As core material often contains material that is hard to penetrate with energy levels below 80kV, we used this energy level for the low energy scans.

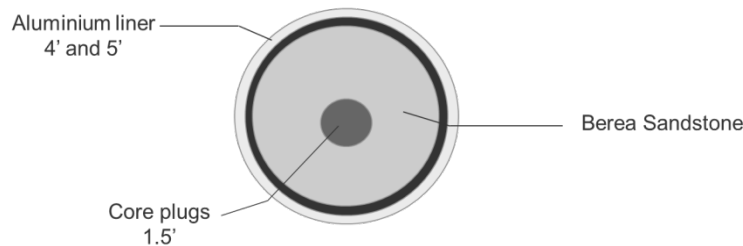


**Figure 1:** Setup for scanning of calibration samples. The calibration samples are placed inside a drilled out hole in a Berea sandstone. The Berea sandstone is placed inside an aluminium liner.

We used a set of calibration samples with large variation in density to obtain values for the unknowns  $\alpha$ ,  $\beta$  and  $\gamma$  in Equation 4. To obtain conditions similar to the actual scanning of core samples, we placed the calibration samples inside a sandstone core sample within an enclosing aluminium liner. For this we drilled out a cylindrical hole with diameter slightly larger than 1.5 inches in the middle of a cylindrical Berea

sandstone. The calibration samples were then placed inside the central hole of the Berea sandstone, as depicted in Figure 1, and then scanned with two energy levels.

This calibration of each parameter ( $\alpha$ ,  $\beta$  and  $\gamma$ ) is unique for each scanner. Source, filters and detectors vary between machines, and such hardware changes affect the resulting CT-values.

### CT image processing:

Evaluation of structural characteristics for different reservoir rocks requires standardization of image quality. In this study, CT scanner hardware settings for dual energy scans have been standardized to obtain reproducible quality irrespective of the scanner type as shown in Table 1.

**Table 1:** Standardized hardware and reconstruction settings for dual energy scans of core samples.

Parameters	Dual Energy	
Voltage (kV)	80	140(or max available)
Effective current (mA)	1800(or max available)	400 (or max available)
Slice thickness (mm)	0.6 (or min available)	
Rotation time (sec)	1 (or max available)	
Pitch	0.35 (or min available)	
Field of view	120 (fit to sample size)	
Protocol (Body part examined)	HEAD	

All the investigated cores are scanned within their liner to avoid any extra damages due to handling, in addition the aluminum envelope then act as an extra X-ray filter. Dicom-format data files are acquired for each scanned core. A python script has been developed to load, crop (to remove the surrounding liner) and export 2D images of the scanned cores automatically.

From the digitized 3D core volumes, we extracted 2 longitudinal slices (XZ and YZ) and an unrolled surface image of each scanned core as shown in Figure 2.

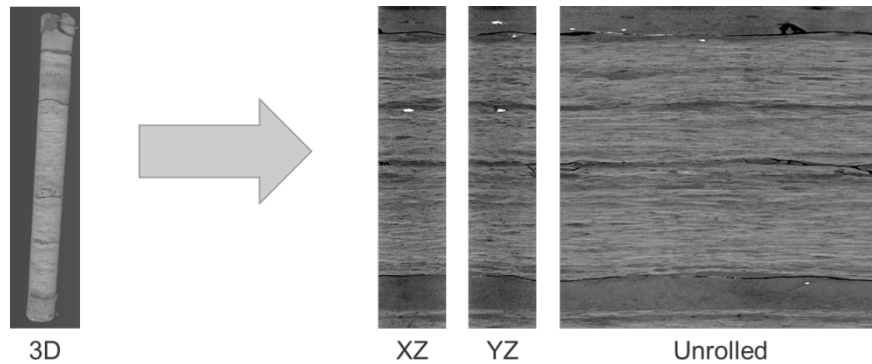


**Figure 2:** Longitudinal slices and unrolled surface are extracted from 3D cropped volume of each core (0.5 mm vertical resolution)

The resulting 2D images (XZ, YZ and unrolled) are then imported as high resolution array data using specially designed scripts within log evaluation software to be further treated as typical image logs. XZ and YZ slices can be directly compared to conventional core pictures and unrolled surface to borehole images.

#### **Alignment and orientation of CT images:**

The unrolled surface of the core originating from the CT scans can then be compared to borehole images. This is used for improving interpretation of borehole image logs (ultrasonic, electrical or density based logs). Cores pulled out to the surface are often not oriented with respect to the formation and to each other. It is important to align the unrolled surface to neighboring (above and below) cores. When image logs are available they can be used to orient the core images accordingly, as shown in Figure 3. In collaboration with Enthought Inc we have developed a set of python libraries for fast alignment and orientation of large intervals of cores. A graphical user interface within VirtualCore © software allows to define chunks of cores to be aligned and further oriented using available borehole image.

For selected intervals where unrolled surfaces have been aligned and oriented, we then export the images as a standard borehole image log (DLIS format) for complete integration in log evaluation software.

Dip amplitude differs between borehole image logs and CT unrolled surface due to diameter difference (larger for image logs) but frequency remains the same as seen in Figure 3 where borehole image log is based on a 8 ½" borehole diameter and the core diameter is 2 ½" after cropping.

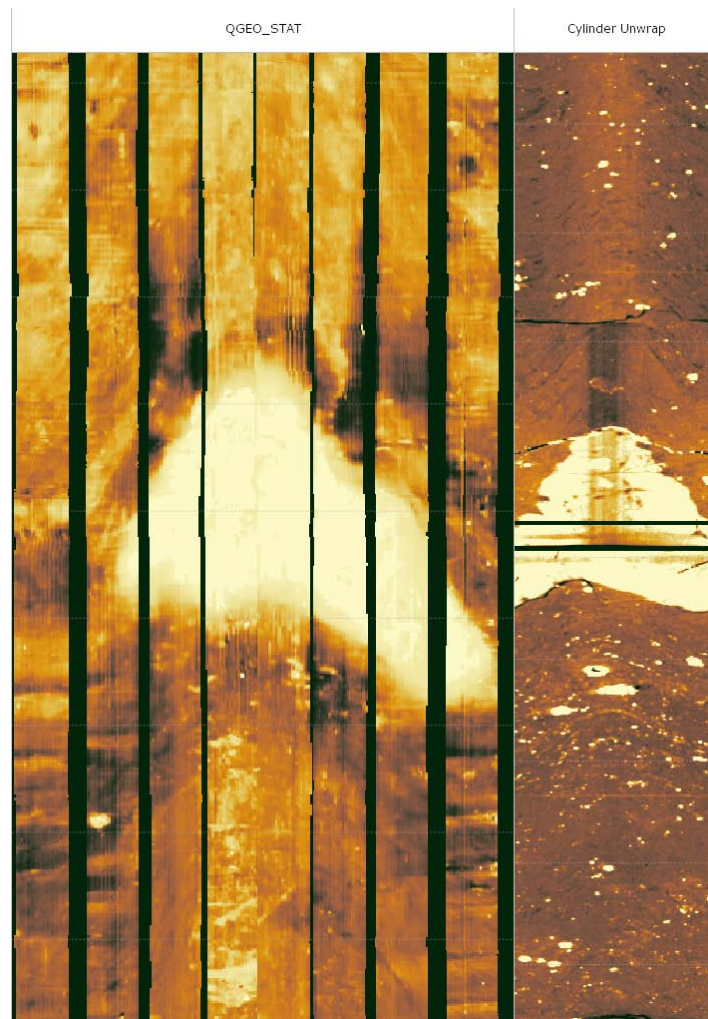


**Figure 3:** 2 meter section of QuantaGeo © borehole imager (left) and corresponding unrolled CT surface of the two 1 meter cores (right) aligned and oriented using VirtualCore software.

## RESULTS

### Calibration of density and PEF calculations:

A set of 12 calibration samples was scanned at 80 and 140kv with a Siemens Definition Edge medical CT-scanner. We then optimized the values for the unknowns  $\alpha$ ,  $\beta$  and  $\gamma$  in Equation 4 to obtain a smallest possible squared error between the calculated from DECT and measured density values (volumetric). The resulting values are shown in Table 2, where we also include the calibrated constants used in Equation 5 for calculation of the photoelectric factor. The calculated densities are plotted versus the measured densities in Figure 4. The plot shows that for the calibration samples the constants in Table 2 gives a good match between measured and calculated values for the density, with all samples

having an error smaller than 2.1%. Note that these parameters are specific for the type of scanner.

**Table 2:** The resulting calibrated constants in Equation (4) and Equation (5) for a Siemens Definition Edge medical CT-scanner.

$\alpha$	$\beta$	$\gamma$
-0.778	1.984	1007.3
$\delta$	$\epsilon$	$\zeta$
36597	-35331	233946

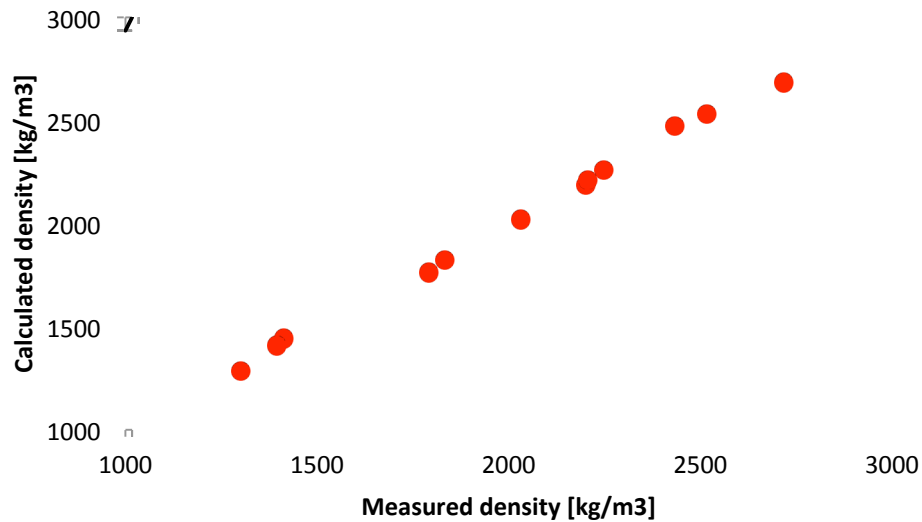


**Figure 4:** Plot comparing calculated and measured densities for the calibration samples. The plot also contains the 1-1 line for comparison.

The calibrated Equation (4) was then applied to a set of reservoir rock samples. These rock samples consisted of both plugs and a whole core. The resulting densities are plotted in Figure 5. As the maximal error was 2.1% for the calibration samples, we have included a 2% error bar in the plot for comparison.

The plot reveals that we have larger uncertainties for the reservoir rock samples than for the calibration sample set. One reason seems to be the presence of matter with high X-ray attenuation. When investigating the samples with the largest error, we found that there were significant parts of the sample where the traversing X-rays were completely attenuated. Even for the 140kV energy level, there were parts of the sample where the X-rays did not penetrate through.



For the full-core sample we tried to scan with two different liner thicknesses. This had minor effect on the calculated values. We also tried to scan water, as the water density is significantly outside the density values used for the calibration. Still we got a resulting density value of 1029 kg/m<sup>3</sup>, which is a fair match to the density of fresh water.

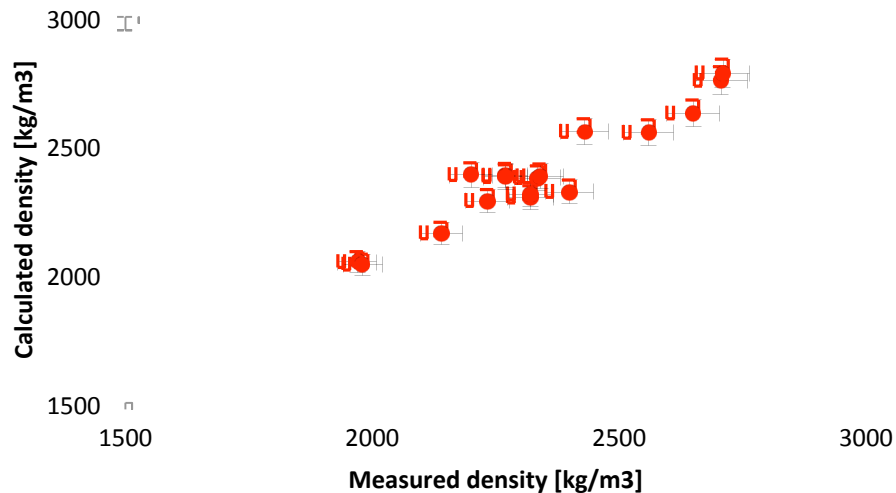


**Figure 5:** Calculated versus measured values for different reservoir rock samples. The plot also contains a 2% error bar for all the samples, and the 1-1 line for comparison.

### Effective core properties:

The investigated whole core CT scans were automatically cropped using python scripts, for enabling automatic calculations of density values. The workflow was tested on several sets of core samples for different production fields.

For the cropped core samples the density was calculated for each pixel using Equation (4), and then averaged per horizontal slice (0.5mm thickness). This resulted in a density log for the scanned interval with a vertical resolution of 0.5mm. From the density log calculated from DECT and based on fluid assumptions, we estimated the total porosity using the Equation (6). The CT derived logs were integrated into log evaluation software and there compared to formation bulk density log from wireline tools.

Typical resolution for a wireline density tool is 30-50 cm, and therefore not suitable for volume estimation in thin bedded reservoirs. In general bulk density from DECT dataset are quite noisy and need to be smoothed and filtered to remove possible artifacts. This leads to a loss of resolution from 0.5mm to 5mm for our dataset.

In Figure 6 we have shown porosity estimates based on density calculations. The plot includes different filtering and smoothing, alongside conventional logs and CT images for a US onshore field. We observe that DECT and wireline porosity are in good agreement, while the DECT porosity gives more insight on the thin beds present for the investigated interval. Combining wireline logs, CT images and DECT derived properties allowed us to re-estimate porosity over the investigated interval.

On the example showed in Figure 6, the well was vertical and neither orientation nor alignment was needed due to mainly horizontal bedding.

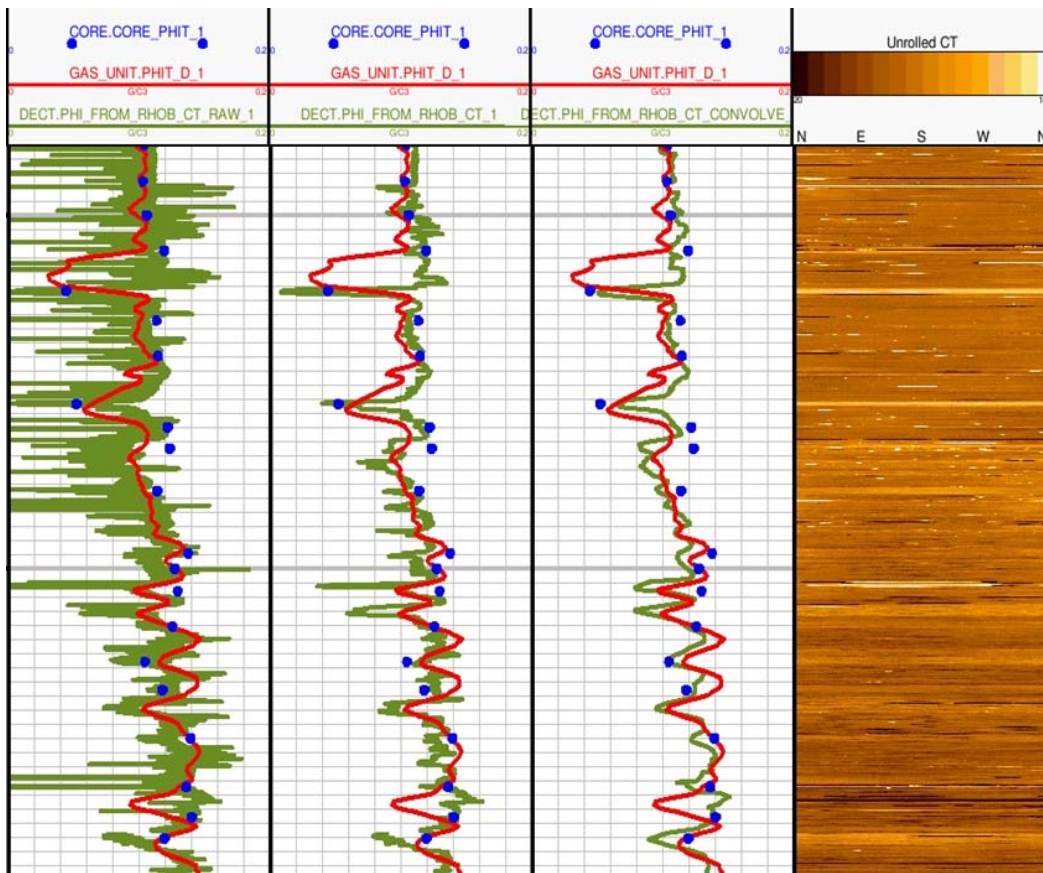


**Figure 6:** Total porosity from wireline log (red), from DECT (green) and core measurement (blue) over more than 100 feet of investigated interval. First column is with raw DECT data, second is with smoothed and filtered DECT data and third column is with DECT data averaged to same resolution as the wireline density tool (0.5m). The fourth column is the corresponding unrolled surface of the imaged core.

### Structural analysis on CT images:

In this study, we have developed python scripts to automatically crop and unroll CT images of whole cores. Unrolled CT images are converted to DLIS file for the

investigated interval and loaded into log evaluation software. Once in log evaluation software unrolled CT images can be treated as regular borehole image from image logs. In Figure 7, we show an example of an oriented unrolled CT image of 3 meters sections core on which fracture orientation is performed. From the corresponding resistivity image logs it is not possible to pick the fracture visible on the CT image. Combining the two logs offer a new insight in formation evaluation.

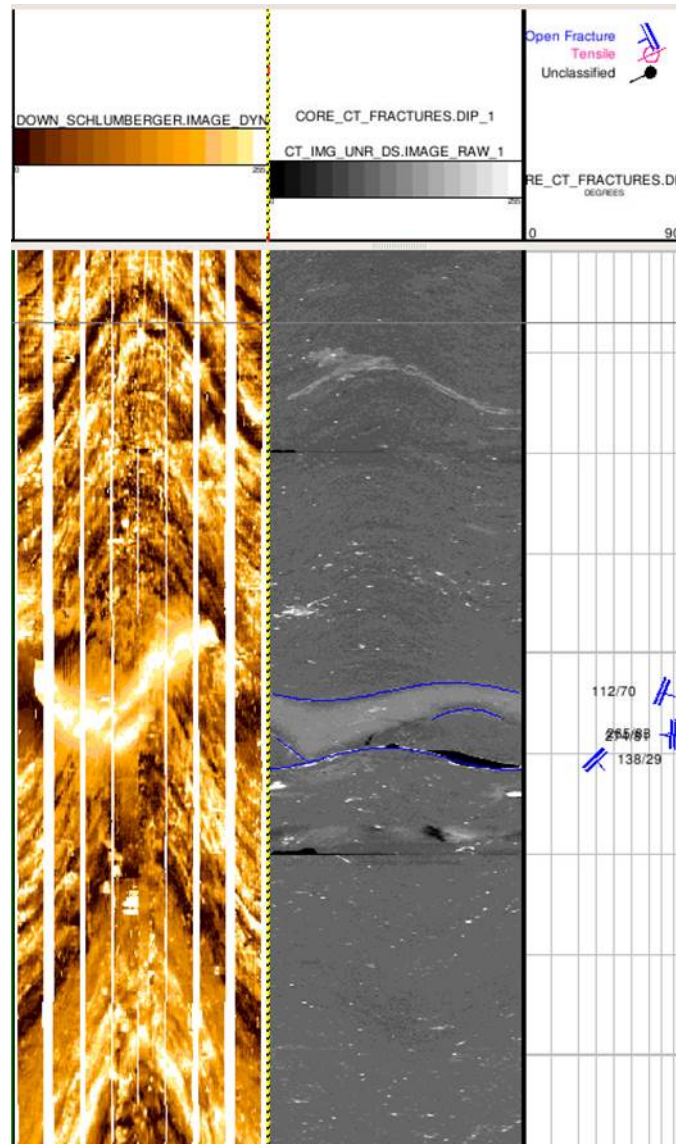


**Figure 7:** Resistivity image log (left) used for orienting unrolled CT image (middle). Fracture picking and orientation is then based on unrolled CT image track.

## CONCLUSION

We have developed a workflow for fast integration of images and calculated properties from dual energy CT-scans of core samples into conventional log evaluation software. Such CT-data can then be used alongside traditional log data for formation evaluation.

In this study we have validated a method to calibrate the equations used for calculation of rock properties,; density and porosity. With standardized scanning experimental design and hardware settings the resulting images and calculated values are comparable for the given scanner irrespective of the investigated interval.

## REFERENCES

1. Cromwell, V., D. J. Kortum, and D. J. Bradley. "The use of a medical computer tomography (CT) system to observe multiphase flow in porous media." SPE Annual Technical Conference and Exhibition. Society of Petroleum Engineers, 1984.
2. Wellington, S. L., and H. J. Vinegar. "X-ray computerized tomography." *Journal of Petroleum Technology* 39.08 (1987): 885-898.
3. Gilliland, R. E., and M. E. Coles. "Use of CT scanning in the investigation of damage to unconsolidated cores." SPE Formation Damage Control Symposium. Society of Petroleum Engineers, 1990.
4. Withjack, E. M., C. Devier, and G. Michael. "The role of X-ray computed tomography in core analysis." SPE Western Regional/AAPG Pacific Section Joint Meeting. Society of Petroleum Engineers, 2003.
5. Hove, A. O., J. K. Ringen, and P. A. Read. "Visualization of laboratory corefloods with the aid of computerized tomography of X-rays." *SPE Reservoir Engineering* 2.02 (1987): 148-154.
6. Akin, S., and A. R. Kovsky. "Computed tomography in petroleum engineering research." Geological Society, London, Special Publications 215.1 (2003): 23-38.
7. Mohamed, Samy Serag El Din, et al. "Whole Core Versus Plugs: Integrating Log and Core Data to Decrease Uncertainty in Petrophysical Interpretation and STOIP Calculations." Abu Dhabi International Petroleum Exhibition and Conference. Society of Petroleum Engineers, 2010.
8. Almarzooq, Anas, et al. "Shale Gas Characterization and Property Determination by Digital Rock Physics." SPE Saudi Arabia Section Technical Symposium and Exhibition. Society of Petroleum Engineers, 2014.
9. Siddiqui, Shameem, and Aon A. Khamees. "Dual-energy CT-scanning applications in rock characterization." SPE Annual Technical Conference and Exhibition. Society of Petroleum Engineers, 2004.